

## Long-term stability study of the passivation quality of polysilicon-based passivation layers for silicon solar cells

Di Kang<sup>a,\*</sup>, Hang Cheong Sio<sup>a</sup>, Di Yan<sup>a</sup>, Wenhao Chen<sup>a</sup>, Jie Yang<sup>b</sup>, Jingsheng Jin<sup>b</sup>, Xinyu Zhang<sup>b</sup>, Daniel Macdonald<sup>a</sup>

<sup>a</sup> Research School of Electrical, Energy and Materials Engineering, The Australian National University (ANU), Canberra, ACT, 0200, Australia

<sup>b</sup> Jinko Solar Co., Ltd, Shangrao, Jiangxi Province, China

### ARTICLE INFO

#### Keywords:

Polysilicon  
Degradation  
Surface passivation  
Czochralski silicon (Cz-Si)  
Float zone silicon (FZ-Si)  
Silicon solar cells

### ABSTRACT

We investigate the stability of the effective lifetime  $\tau_{eff}$  and the recombination current density parameter  $J_0$  in n-type silicon samples with symmetric phosphorus doped poly-Si/SiO<sub>x</sub> structures, and identify factors that contribute to the passivation degradation behavior. It is found that the surface passivation quality of phosphorus doped polysilicon passivating contacts degrades upon dark annealing and light soaking at temperatures between 75 °C and 200 °C, which can lead to a pronounced increase of the recombination current density parameter  $J_0$  (one-side) from below 10 fA/cm<sup>2</sup> to 50 fA/cm<sup>2</sup> or above. The degradation is only detected on fired wafers, whereas the surface passivation quality is found to be stable in the non-fired sister samples. Surprisingly, a recovery of  $\tau_{eff}$  and  $J_0$  is observed after the degradation. The degradation and regeneration behaviors depend strongly on temperature and light intensity, and the presence of silicon nitride (SiN<sub>x</sub>) capping layers during the light soaking. Increasing the annealing temperature dramatically increases the rate of the degradation and the regeneration process, and at the same time reduces the magnitude of the degradation. The regeneration process appears to be affected by the presence of SiN<sub>x</sub> films during the light soaking treatment. Samples with SiN<sub>x</sub> films removed after firing suffer a significantly larger degradation upon light soaking without any lifetime regeneration. Grazing incidence X-ray diffraction measurements reveal negligible change in the structural property and crystalline quality of the polysilicon layer during the degradation.

### 1. Introduction

Recombination losses at metal-silicon interfaces are a key factor limiting the efficiencies of industrial crystalline silicon (c-Si) solar cells [1]. One approach to limit this loss mechanism is to reduce the contact fraction using local contacts. Devices with such structures, such as the passivated emitter and rear cells (PERC), show improved performance [2]. Alternatively, passivating contact structures have been found to be efficient in reducing carrier recombination at the contact regions, while allowing effective carrier-selective contacts for solar cells [3,4].

Among the various passivating contact technologies, polysilicon (poly-Si) passivating contacts, consisting of an ultra-thin SiO<sub>x</sub> layer capped with a doped poly-Si film, show great potential to be used for high efficiency devices in mass production [5,6]. It has been demonstrated that the application of phosphorus poly-Si and SiO<sub>x</sub> as a carrier selective full-area rear contact can lead to a significant efficiency improvement in n-type solar cells [7–9]. Mass production of solar cells

with POCl<sub>3</sub> diffused poly-Si passivating rear contacts is already underway, and it is expected that the technology will gain significant market share in the near future [10].

Although poly-Si passivating technologies have been extensively studied, the majority of previous work has been focused on their electrical performance directly after fabrication [3,11–15]. Unlike the reliability studies on passivated emitter and rear cells (PERC) [16–20], few studies have been performed on the longer-term stability of poly-Si passivation structures upon illumination and annealing. An exception is the study by Winter et al. [21] who recently reported that phosphorus doped poly-Si passivation layers applied on both p- and n-type Czochralski silicon (Cz-Si) substrates exhibit a firing-related degradation and recovery phenomenon when subjected to either illumination or dark annealing. Moreover, Yang et al. [22] reported changes in surface passivation in Cz-Si samples featuring phosphorus doped poly-Si upon light soaking or dark annealing at above 150 °C, and an improvement in surface passivation was observed on samples light soaked or annealed at

\* Corresponding author.

E-mail address: [di.kang@anu.edu.au](mailto:di.kang@anu.edu.au) (D. Kang).

temperatures above 250 °C.

This work further investigates the long-term stability (up to 100,000 min or 70 days) of phosphorus doped poly-Si passivation layers on n-type silicon substrates under illumination at elevated temperature, and explores the impact of several factors, including the degradation conditions (temperature and light intensity), poly-Si fabrication processes, firing profile, the properties of SiN<sub>x</sub> films, and the presence or absence of SiN<sub>x</sub> capping layers during the light soaking. The samples were characterized by effective lifetime ( $\tau_{eff}$ ), recombination current density parameter ( $J_0$ ) and implied open-circuit voltages ( $iV_{oc}$ ), to respectively demonstrate the overall electronic degradation behavior, the corresponding changes in the surface passivation quality, and the potential influence on device performance. A room temperature super-acid passivation technique [23] was applied to monitor any variations in the bulk lifetimes of the samples during the stability experiments. Finally, we compare the degradation behaviors of ex-situ doped (through POCl<sub>3</sub> diffusion) poly-Si passivation layers fabricated via two different silicon film deposition approaches, the Plasma Enhanced Chemical Vapor Deposition (PECVD) approach and the Low Pressure Chemical Vapor Deposition (LPCVD) approach. Those two approaches are considered as the two main technologies for silicon films deposition in industrial mass production [10,24].

## 2. Experimental details

**Fig. 1** shows a flowchart outlining the experimental details. The samples feature a symmetric phosphorus doped poly-Si/SiO<sub>x</sub> structure and SiN<sub>x</sub> capping layers on both surfaces. PECVD and LPCVD poly-Si layers were separately prepared on n-type phosphorus doped float-zone (FZ) and Cz-Si wafers. Samples passivated by PECVD poly-Si layers were prepared in our lab at ANU, using processes outlined in our previous works [15,25] for manufacturing high-efficiency poly-Si devices. The FZ-Si wafers had a resistivity of 2 Ω cm and a thickness of 300 ± 10 μm. After saw damage etching, thin thermal oxide layers were grown on the FZ samples by submerging them in boiling nitric acid solution for 30 min. A 50 nm thick intrinsic a-Si layer was then deposited on both sides of the wafers using a Roth and Rau AK400 PECVD tool, followed by a thermal POCl<sub>3</sub> diffusion at 840 °C to dope and crystallize the poly-Si film, and then a forming gas anneal at 400 °C for 30 min. Afterwards, the FZ-Si samples were coated with SiN<sub>x</sub> films deposited using an Oxford PlasmaLab 100 PECVD system, and fired in a rapid thermal process (RTP) furnace at 700 °C (actual temperature) for 5 s with a ramp up and cool down rate of 20 °C/s and 70 °C/s (average rate from peak firing temperature to 400 °C) respectively. The n-type Cz-Si wafers had a resistivity of 4 Ω cm and a thickness of 180 ± 5 μm. The planar Cz-Si wafers were processed similarly to the FZ-Si samples described above, but with different equipment in an industrial

production line. In particular, 100 nm intrinsic a-Si layers were deposited on the Cz-Si samples with an LPCVD tool and doped by phosphorus diffusion, as compared to the PECVD tool used for the FZ-Si samples. Three different SiN<sub>x</sub> films were deposited on the LPCVD deposited poly-Si films samples, either using an Oxford PlasmaLab 100, a Roth and Rau AK400, or a Centrotherm batch-type PECVD tool, to study the potential influence of the SiN<sub>x</sub> capping layer. The samples with LPCVD poly-Si were then fired at various temperatures either in a conveyor belt furnace (with a measured peak temperature of 770 ± 30 °C) or in an RTP furnace (with actual peak firing temperature of 600 °C, 700 °C, or 750 °C). In order to identify the factors affecting degradation behaviors, samples were divided into several groups according to the fabrication methods and degradation conditions. **Table 1** summarizes the key differences in processing steps of samples in each group.

The degradation tests were performed on a hotplate at various temperatures under illumination by a white light emitting diode (LED) light source with illumination intensity varying between 0.1 and 1 sun. During the tests,  $\tau_{eff}$  and  $iV_{oc}$  values were measured using a Sinton Instruments WCT-120 QSSPC at room temperature [26].  $J_0$  values were also extracted using the Kane and Swanson method [27] to monitor changes in the surface passivation quality of poly-Si passivation layers. To evaluate the bulk lifetimes of the samples, a super-acid passivation technique was employed [23,28]. We selected various samples at different degradation stages, removed their surface films (SiN<sub>x</sub> and poly-Si/SiO<sub>x</sub>) via HF dip and TMAH etch, and then measured the lifetimes of the samples with a room-temperature passivation treatment using a super-acid solution mixed by bis(trifluoromethane)sulfonimide (TFSI) and hexane. It is noted that the heavily doped phosphorus diffused region in the crystalline silicon bulk near the surface was also removed during the TMAH etch, which removed around 5 μm from each surface of the wafers.

The structural properties of the poly-Si thin films before and after the degradation tests were examined by grazing incidence X-ray diffraction (GIXRD) measurement. The SiN<sub>x</sub> layers were removed from the samples by hydrogen fluoride (HF) solution prior to the GIXRD characterization. A PANalytical X'Pert PRO MRD High Resolution X-ray diffractometer with CuKα radiation and a graphite monochromator was used.

## 3. Results and discussion

### 3.1. Overall degradation behaviors

**Fig. 2** shows the evolution of  $\tau_{eff}$  measured at an injection level of  $1 \times 10^{15} \text{ cm}^{-3}$ , and the corresponding  $J_0$  values (for one side) in the industrially-processed LPCVD poly-Si passivated n-type Cz-Si samples under 1-sun illumination at 140 °C. The  $J_0$  values were extracted using the Kane and Swanson method [27], based on lifetime values at injection levels between  $3.5 \times 10^{15}$  and  $9.5 \times 10^{15} \text{ cm}^{-3}$ . **Fig. 2** (b) shows examples for  $J_0$  fittings measured at initial (before degradation) and maximum degradation stages. A linear correlation between  $(1/\tau_{eff} - 1/\tau_{Auger})$  and  $\Delta n$  was observed, demonstrating the accuracy of the extracted  $J_0$  values [31]. Note that the samples are assumed to have identical poly-Si films on the front and the rear side, and the single-side  $J_0$  values were obtained by dividing the extracted  $J_0$  by 2. As seen in **Fig. 2** (a) and (b), an obvious reduction in  $\tau_{eff}$  and a corresponding increase in  $J_0$  is detected in the sample. Interestingly, a partial recovery in  $\tau_{eff}$  and  $J_0$  can be observed after 10,000 min of illumination. The reduction and recovery of  $J_0$  correlate well with the changes of effective lifetimes, indicating that the degradation is likely to be due to variations in surface passivation quality.

To differentiate the bulk contribution to the observed degradation phenomena, we measured lifetimes with room-temperature super-acid passivation treatment [23], on sister samples collected at different degradation stages during the light soaking under 1 sun at 140 °C (show in **Fig. 2** (a)), after removing their surface films (SiN<sub>x</sub> and poly-Si/SiO<sub>x</sub>). It is notable that lifetimes measured with super-acid treatment are not

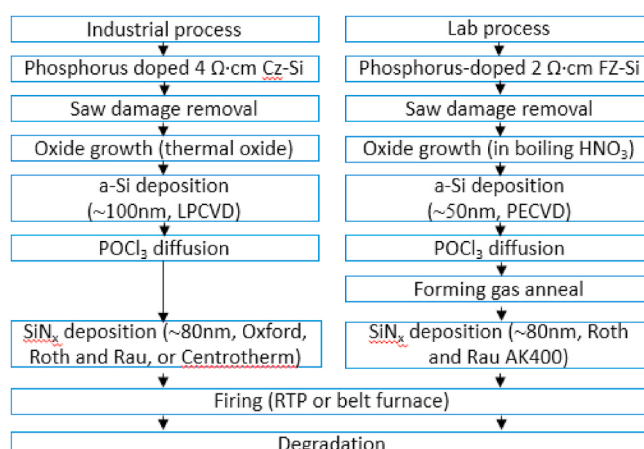


**Fig. 1.** Flowchart of experimental details.

**Table 1**

Descriptions of processing steps and degradation conditions studied in this work.

	Process <sup>a</sup>	SiN <sub>x</sub> films <sup>b</sup>	Firing condition	Degradation temperature	Light intensity
Overall degradation behaviors (Section 3.1)	Industrial	III	Belt furnace <sup>c</sup>	140 °C	1 sun
Dependence on degradation temperatures (Section 3.2)	Industrial	III	Belt furnace <sup>c</sup>	75 °C, 140 °C, or 200 °C	1 sun
Dependence on illumination intensities (Section 3.3)	Industrial	III	Belt furnace <sup>c</sup>	200 °C	0.1 suns, 0.5 suns, 1 sun, or dark anneal
Dependence on fabrication processes (Section 3.4)	Industrial	III	Belt furnace <sup>c</sup>	140 °C	1 sun
Dependence on firing profiles (Section 3.5)	Lab	II	RTP 700 °C		
Dependence on SiN <sub>x</sub> films (Section 3.6)	Industrial	III	RTP: 600 °C, 700 °C, or 750 °C; Belt furnace <sup>c</sup>	140 °C	1 sun
		II	RTP 750 °C	140 °C	
			RTP 750 °C	200 °C	

<sup>a</sup> The processing steps are outlined in Fig. 1. Note that, as illustrated in Fig. 1, different Si wafers were used for industrial and lab processed samples.

<sup>b</sup> SiN<sub>x</sub> I, II and III denotes silicon nitride films deposited using an Oxford PlasmaLab 100, a Roth and Rau AK400, or a Centrotherm batch-type PECVD tool respectively.

<sup>c</sup> Belt furnace firing process denotes a conventional industrial firing profile with an actual peak firing temperature of 770 ± 30 °C.

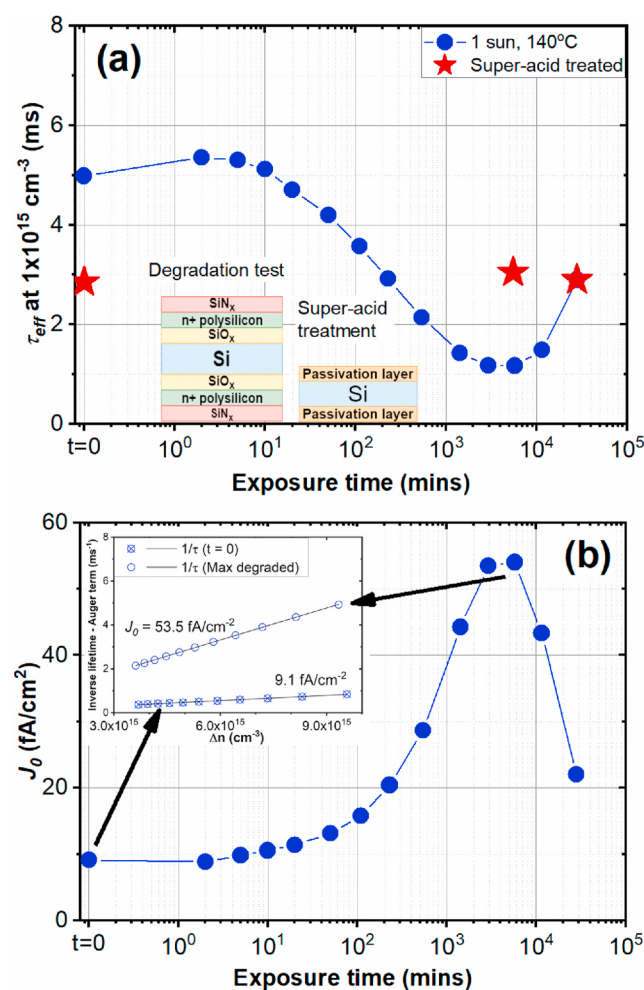


**Fig. 2.** Evolution of (a)  $\tau_{eff}$  and (b)  $J_0$  for samples illuminated under 1 sun at 140 °C. Also presented in Fig. 2 (a) are lifetimes measured by super-acid treatment [23] on samples collected at various degradation stages, including before light soaking, at the maximum degradation stage, and after a slight recovery. Inverse lifetimes ( $1/\tau_{eff} - 1/\tau_{Auger}$ ) as a function of excess carrier density  $\Delta n$  for the sample measured at two different degradation stages are shown in Fig. 2 (b), and  $J_0$  values are determined from the slope of the fit ( $\Delta n$  ranging from  $3.5 \times 10^{15}$  to  $9.5 \times 10^{15} \text{ cm}^{-3}$ ). The samples, as shown in Table 1, were industrially sourced and fired by belt furnace at a peak firing temperature of  $770 \pm 30$  °C (actual temperature). The lines are guides to the eye.

necessarily the actual bulk lifetime of the wafers, as they are partly limited by the passivation quality of the super-acid solution, limiting  $\tau_{eff}$  to around 3 ms in this case. However, comparing the lifetime values of samples passivated from the same batch of super-acid treatment can reveal changes in the bulk properties. As shown in Fig. 2 (a), the measured lifetimes are almost constant during the light soaking, confirming that the observed degradation in the effective lifetimes of the sample is caused by changes in the surface passivation quality. A further evidence for the degradation to occur in surface passivation rather than in the bulk is that the injection dependence of the  $\tau_{eff}$  after degradation is consistent with a change in the  $J_0$  parameter, with minimum lifetime reduction detected at low-injections. This leads to a conclusion that this degradation phenomenon is different from the widely reported light and elevated temperature induced degradation (LeTID), which is known to be a bulk-related degradation [20,29,30].

We compare the structural properties and crystalline quality of the poly-Si films before and after light soaking with GIXRD, to investigate its potential correlation with the observed degradation behaviors. The degraded sample was exposed to 1 sun illumination at 140 °C conditions for around 5000 min to achieve the maximum degraded state. As shown in Fig. 3, there is negligible change in the diffraction pattern from samples before and after the degradation, suggesting the degradation is not likely due to changes in the degree of crystallization, such as an increase in crystal grain size.

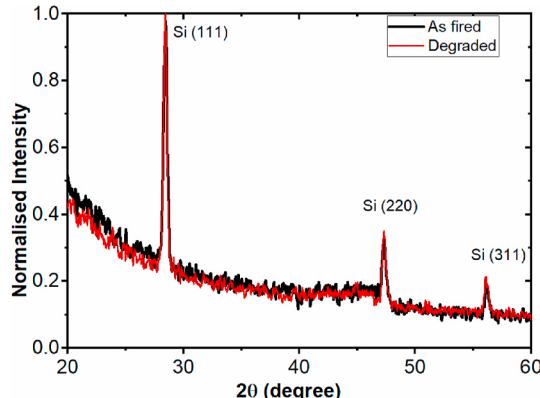


**Fig. 3.** Normalized GIXRD spectra of as-fired and degraded samples. SiN<sub>x</sub> films on both samples were removed by HF dip before GIXRD. The degraded sample was exposed under 1 sun at 140 °C for around 5000 min, reaching the maximum degradation condition.

### 3.2. Correlation between degradation behaviors and degradation temperatures

**Fig. 4** compares the samples subjected to light soaking at different temperatures. Samples illuminated at higher temperature (e.g. 200 °C) exhibit faster degradation, but with lower magnitude. The degradation can already be observed on the sample illuminated at 75 °C. However, due to the slow degradation rate at 75 °C, the tested sample does not appear to have reached its maximum degraded state within our experimental timeframe (more than 1500 h). The observed degradation phenomenon in the poly-Si structures can potentially affect the long-term performance of PV modules, and due to its slow reaction rate, might not be detected with standard degradation tests. On the other hand, for the sample degraded under 1 sun at 200 °C, a full recovery of lifetime and  $J_0$  (**Fig. 4 (b)**) can be observed after 2000 min of light soaking. For further investigation in this work, we employed 140 °C and 200 °C for the degradation tests to accelerate the degradation and regeneration process.

It is notable that there is a slight variation in the initial lifetimes and  $J_0$  values in the samples, potentially due to non-uniformity in the processing, such as the phosphorus diffusion. After the first few minutes of illumination, a small lifetime improvement can be also observed in samples, most likely due to the variation in bulk properties, which is evident from stable  $J_0$  values, and the injection dependence of the lifetimes where a larger difference of  $\tau_{eff}$  is detected at low injection (shown in **Fig. 4 (a)**). It is found that the magnitude of the  $\tau_{eff}$  improvement within the first few minutes varies with the degradation conditions. The underlying mechanism for the bulk lifetime improvement remains unclear and is still under investigation.

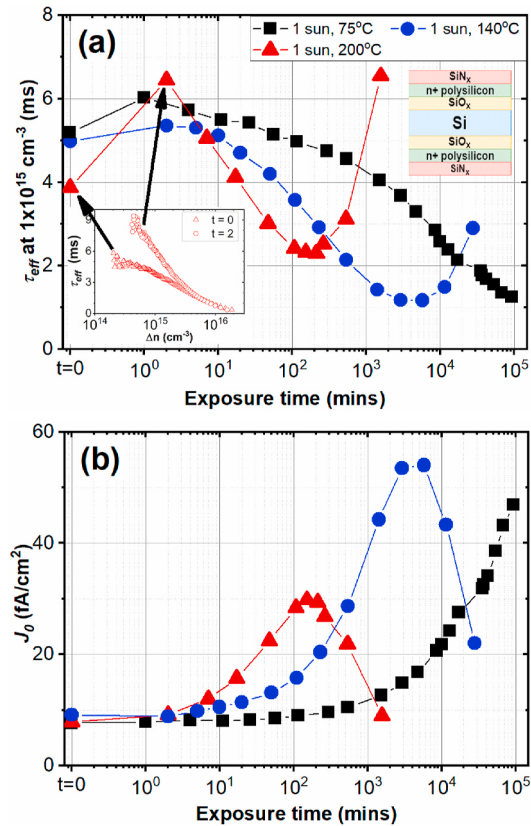


**Fig. 4.** Comparison of degradation behavior for different degradation temperatures with 1-sun light soaking - (a)  $\tau_{eff}$  measured at an injection level of  $1 \times 10^{15} \text{ cm}^{-3}$ , (b) single-side  $J_0$  values. The lines are guides to the eye. Also shown in **Fig. 4 (a)** are injection-level dependent effective lifetimes for the first two measurements of the sample illuminated at 200 °C.

### 3.3. Correlation between degradation behaviors and illumination intensities

The dependence of the degradation behavior on illumination intensity and wavelength is demonstrated in **Fig. 5**. Comparing the degradation behaviors of samples exposed to different light intensities (0.1, 0.5 and 1 sun), the degradation magnitude and rate increase slightly as the light intensity rises. In addition to a white LED light source (correlated color temperature of around 4000 K), we also applied an infrared light source (850 nm) with similar photon flux (estimated by the output current from a reference solar cell) to further investigate the influence of the illumination spectrum. The two samples exposed to infrared and white LED illumination show almost identical degradation rate and magnitude. On the other hand, samples annealed in the dark at 200 °C also show some degradation, but with a considerably slower degradation rate and a lower maximum degradation magnitude, when compared to the sister samples degraded under 1 sun at 200 °C. The almost identical degradation kinetics upon light soaking with different illumination sources, together with the degradation behavior upon dark annealing, imply that ultraviolet (UV) damage [32,33] is unlikely to be the root cause of the observed degradation phenomenon.

Winter et al. [21] also observed degradations in surface passivation quality of phosphorus doped poly-Si passivation layers when samples subjected to dark annealing at 200 °C or illumination at 185 °C. For samples annealed at 200 °C in dark, Winter et al. reported a  $J_0$  change from  $\sim 16 \text{ fA/cm}^2$  to  $\sim 75 \text{ fA/cm}^2$  after 20 h. The degradation is more severe, in terms of both the rate and the magnitude, when compared with our results where  $J_0$  increased from  $\sim 10 \text{ fA/cm}^2$  to  $\sim 20 \text{ fA/cm}^2$  after 6000 min (or 100 h) of dark annealing. For the illuminated samples, the literature presented that, under 1 sun illumination at 185 °C,  $J_0$  increased from  $\sim 16 \text{ fA/cm}^2$  to  $\sim 70 \text{ fA/cm}^2$  to reach its maximum value

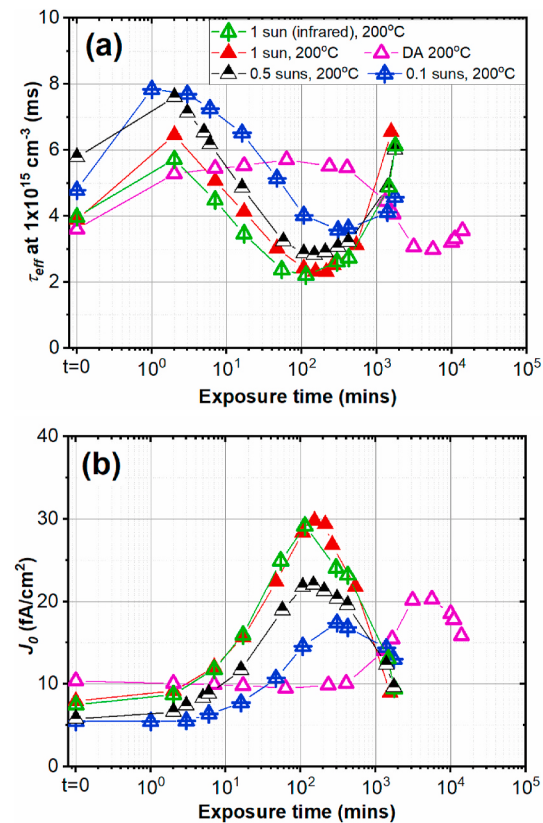


**Fig. 5.** Comparison of degradation behavior tested at 200 °C for various light intensities and different illumination spectrums - (a)  $\tau_{eff}$  measured at injection level of  $1 \times 10^{15} \text{ cm}^{-3}$ , (b)  $J_0$  upon light soaking and dark annealing. The lines are guides to the eye.

in 30 h, which appears a lower degradation speed but higher magnitude compared to the change of  $J_0$  from  $\sim 8 \text{ fA/cm}^2$  to  $\sim 30 \text{ fA/cm}^2$  observed in our sample after 2 h illumination under 1 sun at  $200^\circ\text{C}$ . The variation in the degradation kinetics could be due to the slight difference in the testing conditions, and also be potentially related the poly-Si or the dielectric films on the samples. The following section explores the influence of the processing conditions and properties of the poly-Si films on the degradation behaviors.

### 3.4. Correlation between degradation behaviors and poly-Si fabrication process

To investigate whether the degradation is only applicable to a particular poly-Si fabrication process, we compare the lifetime stability in the industrially processed LPCVD poly-Si films with PECVD poly-Si films processed in our lab at ANU. The results are demonstrated in Fig. 6. These samples feature a similar phosphorus doped poly-Si passivation layer structure, but were fabricated with different tools and processing conditions, coated with different  $\text{SiN}_x$  capping layers, and annealed with different firing profiles either with a belt furnace or an RTA furnace (with processing conditions outlined in Fig. 1 and Table 1). Lab processed wafers have thinner poly-Si layers ( $\sim 50 \text{ nm}$ ) compared to the industrial samples ( $\sim 100 \text{ nm}$ ), enabling us to examine if the degradation is limited to thick poly-Si films. It is noted that the LPCVD poly-Si films were deposited on Cz-Si substrates, whereas FZ-Si substrates were used for the PECVD poly-Si process. Since the changes in  $\tau_{eff}$  and  $J_0$  are mainly attributed to the surface passivation quality as illustrated in Section 3.1 above, we expect negligible influence of the wafer type (n-Cz and n-FZ) on the overall conclusion.

Both PECVD and LPCVD poly-Si films show significant lifetime reduction upon light soaking under 1-sun illumination at  $140^\circ\text{C}$ . The

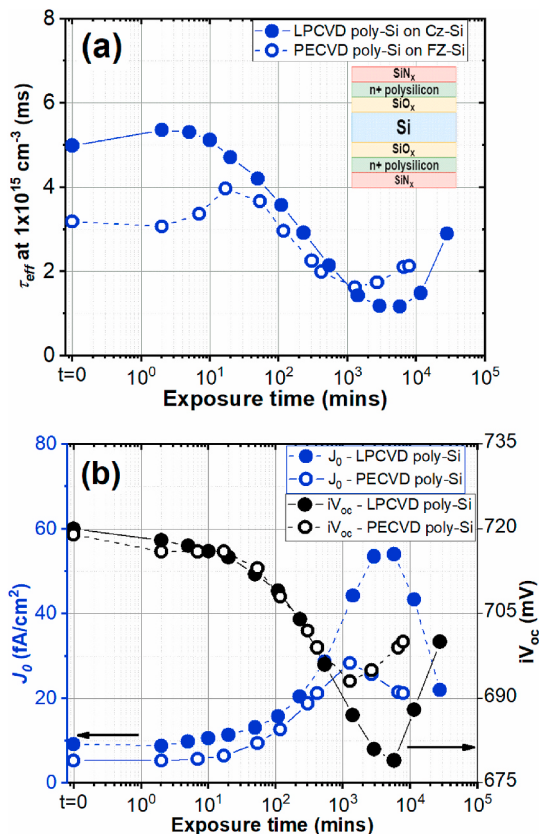


**Fig. 6.** Changes in (a)  $\tau_{eff}$ , (b)  $J_0$  and  $iV_{oc}$  of LPCVD and PECVD poly-Si films under 1-sun illumination at  $140^\circ\text{C}$ . The lifetimes were measured at injection level of  $1 \times 10^{15} \text{ cm}^{-3}$ . The lines are guides to the eye.

measured  $J_0$  values increased significantly, from  $\sim 9 \text{ fA/cm}^2$  to  $\sim 54 \text{ fA/cm}^2$ , and  $5 \text{ fA/cm}^2$  to  $30 \text{ fA/cm}^2$  for the LPCVD and PECVD poly-Si films respectively. This observation, in combination with the results recently presented by Winter et al. [21], suggests that the unstable surface passivation could be a feature of poly-Si structures in general. This degradation phenomenon leads to a substantial reduction in the  $iV_{oc}$  of the samples (shown in Fig. 6 (b)), dropping from 720 mV to 695 mV for the PECVD poly-Si films, and 720 mV–680 mV for the LPCVD films. The results highlight the importance of considering this potential degradation effect when adopting solar cells with poly-Si passivating contacts in mass production.

Moreover, the two types of poly-Si films exhibit different degrees of degradation when exposed to the same testing conditions, implying that the degradation behaviors might be partly related to the sample preparation processes, and are possibly affected by the properties of the poly-Si layers, such as thickness, doping level and crystallinity, or the  $\text{SiN}_x$  films, as well as the firing profiles. These factors are investigated below in Sections 3.5 and 3.6.

### 3.5. Correlation between degradation behaviors and firing profile

Fig. 7 illustrates the influence of the firing profile on the degradation behavior of the industrial poly-Si samples (coated with same  $\text{SiN}_x$  films) under 1-sun illumination at  $140^\circ\text{C}$ . The samples were heated to a peak firing temperature of  $600^\circ\text{C}$ ,  $700^\circ\text{C}$  and  $750^\circ\text{C}$  for 5 s respectively with a  $20^\circ\text{C/s}$  ramp-up rate, and then cooled down to room temperature with a rate of  $70^\circ\text{C/s}$ . A sample fired in a belt furnace, employing a conventional firing profile (actual peak firing temperature of  $770 \pm 30^\circ\text{C}$ ) used for solar cell fabrication, is also included. We have observed similar degradation behaviors on samples fired at  $700^\circ\text{C}$  and  $750^\circ\text{C}$  in an RTP

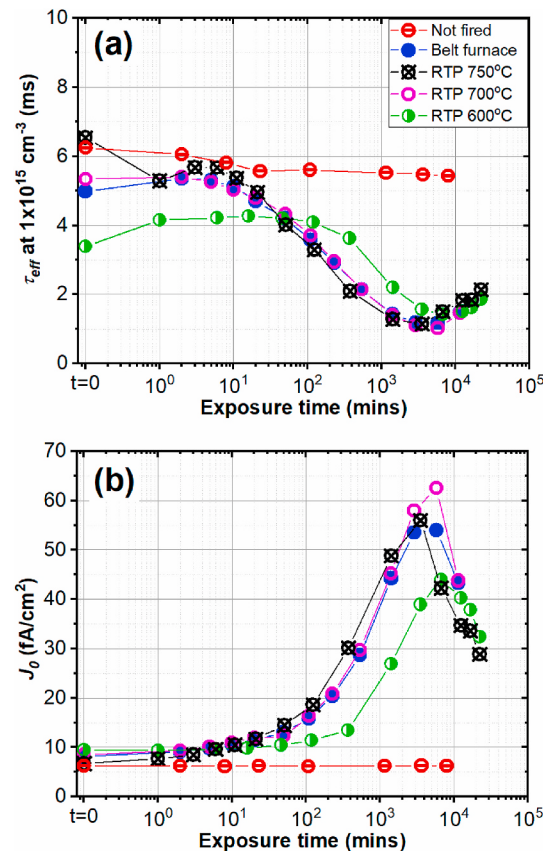


**Fig. 7.** Relationship between degradation behaviors under 1-sun illumination at  $140^\circ\text{C}$  and the firing profile applied. Changes of (a)  $\tau_{eff}$  at  $1 \times 10^{15} \text{ cm}^{-3}$ , and (b)  $J_0$  during light soaking. The lines are guides to the eyes.

furnace and the sample fired with an industrial belt furnace. On the other hand, the sample fired at 600 °C shows slightly less degradation. Interestingly, samples not subjected to the firing treatment appear to be stable during light soaking, suggesting that the degradation behaviors are firing triggered. Our result echoes some previous works on other passivation films, such as SiN<sub>x</sub> and AlO<sub>x</sub> [34,35], where a similar dependence between firing and the long-term instability of the films are reported.

In Fig. 7 (a), it is found that the non-fired sample has a relatively higher  $\tau_{eff}$  compared to the fired wafers (except the sample fired at 750 °C with RTP). The different starting  $\tau_{eff}$  values could possibly be related to inhomogeneity induced by the processing as stated in the previous section, or the firing instability of the TOPCon/SiN<sub>x</sub> structure, as reported by Feldmann et al. [36].

### 3.6. Correlation between degradation behavior and SiN<sub>x</sub> film properties

The degradation and recovery phenomena in poly-Si observed in this study share some similarity with LeTID effects commonly observed on p-type boron-doped mc-Si [16,37–42], particularly in terms of the role of firing [43,44]. It has been demonstrated that LeTID behavior is strongly sensitive to the SiN<sub>x</sub> film properties [42,45]. Here, we compare the degradation behavior in our poly-Si samples capped with SiN<sub>x</sub> films deposited by three different PECVD tools, where these SiN<sub>x</sub> films were found to lead to distinct LeTID behaviors in our previous study [46]. The difference in their degradation behavior is depicted in Fig. 8. It can be observed that the three studied SiN<sub>x</sub> films all yield obvious degradation, but with slightly different kinetics. The film deposited with a Roth and Rau AK400 (SiN<sub>x</sub> - II) leads to the highest increase of  $J_0$  values, and

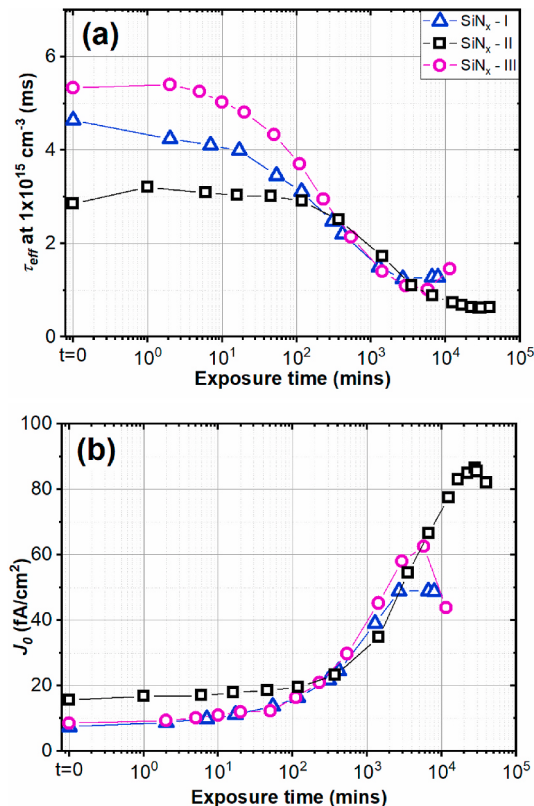


**Fig. 8.** Influence of SiN<sub>x</sub> films on degradation activities under 1 sun illumination at 140 °C. Changes of (a)  $\tau_{eff}$  at  $1 \times 10^{15} \text{ cm}^{-3}$ , and (b)  $J_0$  during light soaking. The three SiN<sub>x</sub> films were of similar thickness, but deposited with different equipment. The lines are guides to the eyes. SiN<sub>x</sub> I, II and III were respectively deposited using an Oxford PlasmaLab 100, a Roth and Rau AK400 or a Centrotherm batch-type PECVD tool.

perhaps surprisingly, this particular SiN<sub>x</sub> film was found not to cause apparent bulk degradation activities in our previous LeTID study [46]. Film densities of the three SiN<sub>x</sub> layers have been found in an order of SiN<sub>x</sub> - I > SiN<sub>x</sub> - III > SiN<sub>x</sub> - II, which are inversely correlated with the degradation in  $J_0$  (shown in Fig. 8 (b)) The correlation could suggest the involvement of hydrogen in the degradation mechanism.

In addition to samples coated with various SiN<sub>x</sub>, samples without SiN<sub>x</sub> capping layers (removed after firing through HF dip) were also studied. It can be observed from Fig. 9 that the samples with and without the SiN<sub>x</sub> capping layers (SiN<sub>x</sub> - II as shown in Fig. 8) show distinct behaviors. Samples capped with SiN<sub>x</sub> during degradation showed a strong degradation and also a full recovery during the test period, whereas the samples without the SiN<sub>x</sub> capping layer exhibited a continuous reduction of lifetime without any sign of recovery. This might suggest that the presence of the SiN<sub>x</sub> layer during the light soaking could play a role in the recovery process, where the SiN<sub>x</sub> films are speculated to perform either as a barrier to avoid hydrogen further effusing from the poly-Si, or as a hydrogen source to inject hydrogen to the poly-Si. This is also supported by the distinct response of various SiN<sub>x</sub> films discussed above in Fig. 8, where denser films act as a more stable hydrogen source or are more effective in preventing the out-diffusion of hydrogen, leading to smaller degradation during light soaking. Note that the non-fired control sample without SiN<sub>x</sub> did not show any lifetime and  $J_0$  changes, in agreement with results discussed above that the degradation is triggered by firing.

As evident in the XRD result discussed above, the observed degradation phenomenon is unlikely to be caused by a change in the crystal properties of the poly-Si structure during the degradation. It is speculated that the degradations or the regenerations afterwards are related to hydrogen, given the fact that a recovery of  $J_0$  is only observable on samples with SiN<sub>x</sub> capping layers, which are known to act as a source of

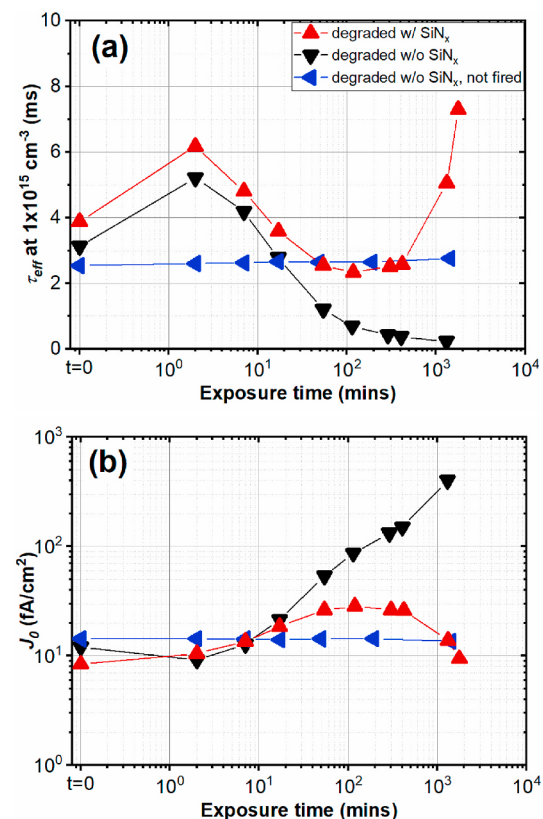


**Fig. 9.** Dependence of SiN<sub>x</sub> film on degradation activities under 1 sun at 200 °C. Changes of (a)  $\tau_{eff}$  at  $1 \times 10^{15} \text{ cm}^{-3}$ , and (b)  $J_0$  in logarithmic scale during light soaking. The samples are coated with SiN<sub>x</sub> - II shown in Fig. 8. The lines are guides to the eyes.

hydrogen [47,48], and also the different degradation kinetics obtained with various  $\text{SiN}_x$  films. Moreover, the degradation observed in this work shares some key similarities to LeTID [43,44,49] and other surface related degradation reported in the literature [35,50], in which the degradation is only detected after firing. This suggests that the defects leading to these degradations could involve the same precursor or could be activated by a similar mechanism, such as the migration of hydrogen [42,51] or a reconfiguration of hydrogen bonding states [52,53]. Interestingly, a recent study by Yang et al. [22] reported a different response on phosphorus doped and boron doped poly-Si structures upon light soaking and dark annealing. Further studies on the difference between  $p^+$  and  $n^+$  poly-Si could provide valuable insight to identify the role of hydrogen in the different passivation structures, and at the same time, to clarify the underlying mechanism for the observed surface degradation.

#### 4. Conclusion

We observed a degradation and recovery of lifetimes in samples with phosphorus doped poly-Si passivating structures upon light soaking at elevated temperature. The  $\tau_{eff}$  trend correlates well with the change of  $J_0$ , and bulk lifetimes in the samples are found to be stable during the test measured by room-temperature super-acid passivation technique, indicating that the lifetime change is due to the instability in the surface passivation quality. Various factors affecting degradation behaviors were investigated, including the degradation conditions, the fabrication equipment (PECVD poly or LPCVD poly), the firing profile and the  $\text{SiN}_x$  capping layers. It was found that the degradation magnitude and rate increase with light intensity and temperature. The degradation is unlikely to be caused by UV damage, as it is also observed upon dark annealing at 200 °C and when the samples are subjected to infrared illumination. Although the degradation is only detected on samples after firing, we did not observe a strong dependence on the firing profile. Samples coated with different  $\text{SiN}_x$  films show only slightly different degradation responses. However, samples without the  $\text{SiN}_x$  capping layer show very severe degradation without any sign of recovery during the test period, suggesting that the presence of  $\text{SiN}_x$  films could play an important role in the regeneration process. Samples before and after degradation were characterized by GIXRD, showing minimal changes in the crystalline properties of the poly-Si films during the degradation. It is suggested that hydrogen is involved in the observed degradation or regeneration phenomena.

#### Declaration of competing interest

The authors declare that they have no known competing financial interests or personal relationships that could have appeared to influence the work reported in this paper.

#### CRediT authorship contribution statement

**Di Kang:** Writing - original draft, Methodology, Conceptualization. **Hang Cheong Sio:** Supervision, Writing - review & editing. **Di Yan:** Formal analysis, Writing - review & editing. **Wenhao Chen:** Data curation. **Jie Yang:** Investigation, Resources. **Jingsheng Jin:** Investigation. **Xinyu Zhang:** Resources, Funding acquisition. **Daniel Macdonald:** Project administration, Writing - review & editing.

#### Acknowledgements

This work has been supported by the Australian Renewable Energy Agency (ARENA) through projects RND017 and 1-A060. Access to the Australian National Fabrication Facility (ANFF) ACT node is gratefully acknowledged.

#### References

- [1] A. Cuevas, P.A. Basore, G. Giroult-Matlakowski, C. Dubois, Surface recombination velocity of highly doped n-type silicon, *J. Appl. Phys.* 80 (6) (1996) 3370–3375.
- [2] M.A. Green, The passivated emitter and rear cell (PERC): from conception to mass production, *Sol. Energy Mater. Sol. Cell.* 143 (2015) 190–197.
- [3] A. Criado, E. Calleja, J. Martinez, J. Piqueras, E. Muñoz, Pn Junction applications and transport properties in polysilicon rods, *Solid State Electron.* 22 (8) (1979) 693–700.
- [4] F. Feldmann, M. Simon, M. Bivour, C. Reichel, M. Hermle, S.W. Glunz, Carrier-selective contacts for Si solar cells, *Appl. Phys. Lett.* 104 (18) (2014) 181105.
- [5] F. Haase, C. Hollermann, S. Schäfer, A. Merkle, M. Rienäcker, J. Krügener, R. Brendel, R. Peibst, Laser contact openings for local poly-Si-metal contacts enabling 26.1%-efficient POLO-IBC solar cells, *Sol. Energy Mater. Sol. Cell.* 186 (2018) 184–193.
- [6] F. Feldmann, M. Bivour, C. Reichel, M. Hermle, S.W. Glunz, Passivated rear contacts for high-efficiency n-type Si solar cells providing high interface passivation quality and excellent transport characteristics, *Sol. Energy Mater. Sol. Cell.* 120 (2014) 270–274.
- [7] A. Rohatgi, B. Rounsville, Y. Ok, A.M. Tam, F. Zimbardi, A.D. Upadhyaya, Y. Tao, K. Madani, A. Richter, J. Benick, M. Hermle, Fabrication and modeling of high-efficiency front junction N-type silicon solar cells with tunnel oxide passivating back contact, *IEEE J. Photovoltaics* 7 (5) (2017) 1236–1243.
- [8] P. Stradins, A. Dameron, S. Essig, V. Lasalvia, B. Lee, Y. Liu, J.-W. Luo, W. Nemeth, A. Norman, M. Page, Passivated Tunneling Contacts to N-Type Wafer Silicon and Their Implementation into High Performance Solar Cells, 2014.
- [9] A. Richter, J. Benick, F. Feldmann, A. Fell, M. Hermle, S.W. Glunz, n-Type Si solar cells with passivating electron contact: identifying sources for efficiency limitations by wafer thickness and resistivity variation, *Sol. Energy Mater. Sol. Cell.* 173 (2017) 96–105.
- [10] Y. Chen, D. Chen, C. Liu, Z. Wang, Y. Zou, Y. He, Y. Wang, L. Yuan, J. Gong, W. Lin, X. Zhang, Y. Yang, H. Shen, Z. Feng, P.P. Altermatt, P.J. Verlinden, Mass production of industrial tunnel oxide passivated contacts (i-TOPCon) silicon solar cells with average efficiency over 23% and modules over 345 W, *Prog. Photovoltaics Res. Appl.* 27 (10) (2019) 827–834.
- [11] B. Nemeth, S.P. Harvey, J.V. Li, D.L. Young, A. Upadhyaya, V. LaSalvia, B.G. Lee, M.R. Page, P. Stradins, Effect of the  $\text{SiO}_2$  interlayer properties with solid-source hydrogenation on passivated contact performance and surface passivation, *Energy Procedia* 124 (2017) 295–301.
- [12] D.L. Young, H.M. Branz, F. Liu, R. Reedy, B. To, Q. Wang, Electron transport and band structure in phosphorus-doped polycrystalline silicon films, *J. Appl. Phys.* 105 (3) (2009) 033715.
- [13] P. Sana, J. Salami, A. Rohatgi, Fabrication and analysis of high-efficiency polycrystalline silicon solar cells, *IEEE Trans. Electron. Dev.* 40 (8) (1993) 1461–1468.
- [14] F. Feldmann, M. Bivour, C. Reichel, H. Steinkeper, M. Hermle, S.W. Glunz, Tunnel oxide passivated contacts as an alternative to partial rear contacts, *Sol. Energy Mater. Sol. Cell.* 131 (2014) 46–50.
- [15] D. Yan, A. Cuevas, J. Bullock, Y. Wan, C. Samundsett, Phosphorus-diffused polysilicon contacts for solar cells, *Sol. Energy Mater. Sol. Cell.* 142 (2015) 75–82.
- [16] K. Ramspeck, S. Zimmermann, H. Nagel, A. Metz, Y. Gassenbauer, B. Birkmann, Light Induced Degradation of Rear Passivated Mc-Si Solar Cells, 27th European Photovoltaic Solar Energy Conference and Exhibition, 2012, pp. 861–865.
- [17] F. Kersten, P. Engelhart, H.-C. Ploigt, A. Stekolnikov, T. Lindner, F. Stenzel, M. Bartzsch, A. Szpath, K. Petter, J. Heitmann, J.W. Müller, Degradation of multicrystalline silicon solar cells and modules after illumination at elevated temperature, *Sol. Energy Mater. Sol. Cell.* 142 (2015) 83–86.
- [18] D. Bredemeier, D. Walter, J. Schmidt, Light-induced lifetime degradation in high-performance multicrystalline silicon: detailed kinetics of the defect activation, *Sol. Energy Mater. Sol. Cell.* 173 (2017) 2–5.
- [19] C. Modanese, M. Wagner, F. Wolny, A. Oehlke, H.S. Laine, A. Inglese, H. Vahlman, M. Yli-Koski, H. Savin, Impact of copper on light-induced degradation in Czochralski silicon PERC solar cells, *Sol. Energy Mater. Sol. Cell.* 186 (2018) 373–377.
- [20] K. Nakayashiki, J. Hofstetter, A.E. Morishige, T.A. Li, D.B. Needleman, M. A. Jensen, T. Buonassisi, Engineering solutions and root-cause analysis for light-induced degradation in p-type multicrystalline silicon PERC modules, *IEEE J. Photovoltaics* 6 (4) (2016) 860–868.
- [21] M. Winter, S. Bordihn, R. Peibst, R. Brendel, J. Schmidt, Degradation and regeneration of n+ doped poly-Si surface passivation on p-type and n-type Cz-Si under illumination and dark annealing, *IEEE J. Photovoltaics* 10 (2020) 1–8.
- [22] Y. Yang, P.P. Altermatt, Y. Cui, Y. Hu, D. Chen, L. Chen, G. Xu, X. Zhang, Y. Chen, P. Hamer, R.S. Bonilla, Z. Feng, P.J. Verlinden, Effect of carrier-induced hydrogenation on the passivation of the poly-Si/SiO<sub>x</sub>/c-Si interface, *AIP Conf. Proc.* 2018 (1) (1999), 040026.
- [23] J. Bullock, D. Kiriya, N. Grant, A. Azcatl, M. Hettick, T. Kho, P. Phang, H.C. Sio, D. Yan, D. Macdonald, M.A. Quevedo-Lopez, R.M. Wallace, A. Cuevas, A. Javey, Superacid passivation of crystalline silicon surfaces, *ACS Appl. Mater. Interfaces* 8 (36) (2016) 24205–24211.
- [24] J.-I. Polzin, F. Feldmann, B. Steinhauser, M. Hermle, S. Glunz, Realization of TOPCon Using Industrial Scale PECVD Equipment, 2018.
- [25] R. Basnet, S.P. Phang, C. Samundsett, D. Yan, W. Liang, C. Sun, S. Armand, R. Einhaus, J. Degoulange, D. Macdonald, 22.6% efficient solar cells with polysilicon passivating contacts on n-type solar-grade wafers, *Solar RRL* 3 (11) (2019), 1900297.

- [26] R.A. Sinton, A. Cuevas, M. Stuckings, Quasi-steady-state photoconductance, a new method for solar cell material and device characterization, in: Conference Record of the Twenty Fifth IEEE Photovoltaic Specialists Conference - 1996, 1996, pp. 457–460.
- [27] D.E. Kane, R.M. Swanson, Measurement of the emitter saturation current by a contactless photoconductivity decay method, in: Proceedings of the IEEE 18th Photovoltaic Specialist Conference, 1985, p. 578.
- [28] A.I. Pointon, N.E. Grant, E.C. Wheeler-Jones, P.P. Altermatt, J.D. Murphy, Superacid-derived surface passivation for measurement of ultra-long lifetimes in silicon photovoltaic materials, *Sol. Energy Mater. Sol. Cell.* 183 (2018) 164–172.
- [29] C. Sen, C. Chan, P. Hamer, M. Wright, U. Varshney, S. Liu, D. Chen, A. Samadi, A. Ciesla, C. Chong, B. Hallam, M. Abbott, Annealing prior to contact firing: a potential new approach to suppress LeTID, *Sol. Energy Mater. Sol. Cell.* 200 (2019) 109938.
- [30] F. Fertig, K. Krauß, S. Rein, Light-induced degradation of PECVD aluminium oxide passivated silicon solar cells, *Phys. Status Solidi Rapid Res. Lett.* 9 (1) (2015) 41–46.
- [31] A. Cuevas, D. Macdonald, Measuring and interpreting the lifetime of silicon wafers, *Sol. Energy* 76 (1) (2004) 255–262.
- [32] M. Tayyib, J.O. Odden, T.O. Saetre, UV-induced degradation study of multicrystalline silicon solar cells made from different silicon materials, *Energy Procedia* 38 (2013) 626–635.
- [33] C.R. Osterwald, J. Pruitt, T. Moriarty, Crystalline silicon short-circuit current degradation study: initial results, in: Conference Record of the Thirty-First IEEE Photovoltaic Specialists Conference, 2005, 2005, pp. 1335–1338.
- [34] D. Sperber, A. Heilemann, A. Herguth, G. Hahn, Temperature and light-induced changes in bulk and passivation quality of boron-doped float-zone silicon coated with SiNx:H, *IEEE J. Photovoltaics* 7 (2) (2017) 463–470.
- [35] K. Kim, R. Chen, D. Chen, P. Hamer, A.C.n. Wenham, S. Wenham, Z. Hameiri, Degradation of surface passivation and bulk in p-type monocrystalline silicon wafers at elevated temperature, *IEEE J. Photovoltaics* 9 (1) (2019) 97–105.
- [36] F. Feldmann, T. Fellmeth, B. Steinhäuser, H. Nagel, D. Ourinson, S. Mack, E. Lohmüller, J.-I. Polzin, J. Benick, J. Rentsch, M. Hermle, S. Glunz, Large Area TOPCon Cells Realized by a PECVD Tube Process, 2019.
- [37] D. Bredemeier, D. Walter, S. Herlufsen, J. Schmidt, Lifetime degradation and regeneration in multicrystalline silicon under illumination at elevated temperature, *AIP Adv.* 6 (3) (2016), 035119.
- [38] P.E.F. Kersten, H.-C. Ploigt, F. Stenzel, K. Petter, T. Lindner, A. Szpath, M. Bartzsch, A. Stekolnikov, M. Scherff, J. Heitmann, J.W. Müller, in: A New Light Induced Volume Degradation Effect of Mc-Si Solar Cells and Modules, 31st European Photovoltaic Solar Energy Conference and Exhibition, 2016, pp. 1830–1834.
- [39] J. Lindroos, K. Petter, K. Sporleder, M. Turek, P. Pachó, M. Rinio, Light beam induced current of light-induced degradation in high-performance multicrystalline Al-BSF cells, *Energy Procedia* 124 (2017) 99–106.
- [40] H. Vahlman, A. Haaralitonen, W. Kwapił, J. Schön, M. Yli-Koski, A. Inglese, C. Modanese, H. Savin, Effect of low-temperature annealing on defect causing copper-related light-induced degradation in p-type silicon, *Energy Procedia* 124 (2017) 188–196.
- [41] D. Chen, P.G. Hamer, M. Kim, T.H. Fung, G. Bourret-Sicotte, S. Liu, C.E. Chan, A. Ciesla, R. Chen, M.D. Abbott, B.J. Hallam, S.R. Wenham, Hydrogen induced degradation: a possible mechanism for light- and elevated temperature-induced degradation in n-type silicon, *Sol. Energy Mater. Sol. Cell.* 185 (2018) 174–182.
- [42] C. Vargas, K. Kim, G. Coletti, D. Payne, C. Chan, S. Wenham, Z. Hameiri, Carrier-induced degradation in multicrystalline silicon: dependence on the silicon nitride passivation layer and hydrogen released during firing, *IEEE J. Photovoltaics* 8 (2) (2018) 413–420.
- [43] R. Eberle, W. Kwapił, F. Schindler, M.C. Schubert, S.W. Glunz, Impact of the firing temperature profile on light induced degradation of multicrystalline silicon, *Phys. Status Solidi Rapid Res. Lett.* 10 (12) (2016) 861–865.
- [44] R. Eberle, W. Kwapił, F. Schindler, S.W. Glunz, M.C. Schubert, Firing temperature profile impact on light induced degradation in multicrystalline silicon, *Energy Procedia* 124 (2017) 712–717.
- [45] D. Bredemeier, D.C. Walter, R. Heller, J. Schmidt, Impact of hydrogen-rich silicon nitride material properties on light-induced lifetime degradation in multicrystalline silicon, *Phys. Status Solidi Rapid Res. Lett.* 13 (8) (2019), 1900201.
- [46] D. Kang, H.C. Sio, X. Zhang, Q. Wang, H. Jin, D. Macdonald, LeTID in p-type and n-type mono-like and float-zone silicon, and their dependence on SiNx film properties, in: 36th European Photovoltaic Solar Energy Conference and Exhibition, Marseille, 2019.
- [47] T.N. Truong, D. Yan, C. Samundsett, R. Basnet, M. Tebyetekerwa, L. Li, F. Kremer, A. Cuevas, D. Macdonald, H.T. Nguyen, Hydrogenation of phosphorus-doped polycrystalline silicon films for passivating contact solar cells, *ACS Appl. Mater. Interfaces* 11 (5) (2019) 5554–5560.
- [48] M. Schnabel, B. Van de Loo, W. Nemeth, B. Macco, P. Stradins, W.M.M. Kessels, D. Young, Hydrogen passivation of poly-Si/SiO<sub>x</sub> contacts for Si solar cells using Al<sub>2</sub>O<sub>3</sub> studied with deuterium, *Appl. Phys. Lett.* 112 (2018), 203901.
- [49] D. Chen, M. Kim, B.V. Stefani, B.J. Hallam, M.D. Abbott, C.E. Chan, R. Chen, D.N. R. Payne, N. Nampalli, A. Ciesla, T.H. Fung, K. Kim, S.R. Wenham, Evidence of an identical firing-activated carrier-induced defect in monocrystalline and multicrystalline silicon, *Sol. Energy Mater. Sol. Cell.* 172 (2017) 293–300.
- [50] D. Sperber, A. Graf, D. Skorka, A. Herguth, G. Hahn, Degradation of surface passivation on crystalline silicon and its impact on light-induced degradation experiments, *IEEE J. Photovoltaics* 7 (6) (2017) 1627–1634.
- [51] T.C. Kho, K.R. McIntosh, J.T. Tan, A.F. Thomson, F.W. Chen, Removal of hydrogen and deposition of surface charge during rapid thermal annealing, in: 2008 33rd IEEE Photovoltaic Specialists Conference, 2008, pp. 1–5.
- [52] S.A. McQuaid, M.J. Binns, R.C. Newman, E.C. Lightowers, J.B. Clegg, Solubility of hydrogen in silicon at 1300 °C, *Appl. Phys. Lett.* 62 (14) (1993) 1612–1614.
- [53] R. Jones, B.J. Coomer, J. Goss, B. Hourahine, A. Resende, The interaction of hydrogen with deep level defects in silicon, *Solid State Phenom.* 71 (2000).